SUPPLEMENTARY MATERIALS FOR PUBLICATION 2

Štach M, Ptáčková P, Mucha M, Musil J, Klener P, Otáhal P.

Inducible secretion of IL-21 augments anti-tumor activity of piggyBac-manufactured chimeric antigen receptor T cells.

Cytotherapy. 2020 Dec;22(12):744-754. doi: 10.1016/j.jcyt.2020.08.005. Epub 2020 Sep 17. PMID: 32950390.

Supplemental Data

Fig. S1

A

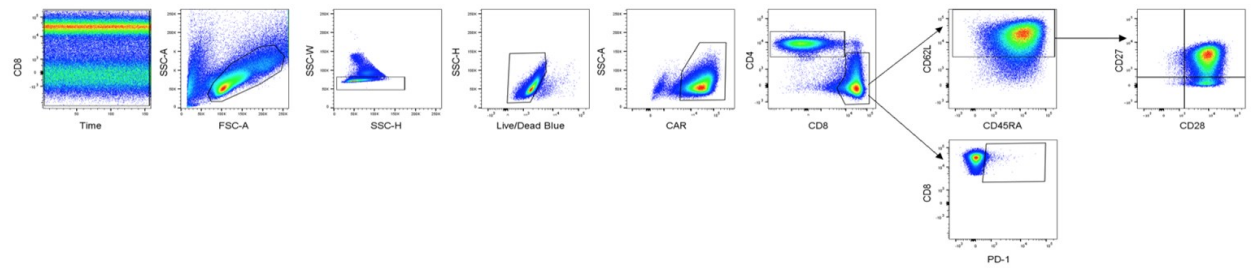

B

The scheme of CAR19 and CAR19 NFAT IL-21 vectors

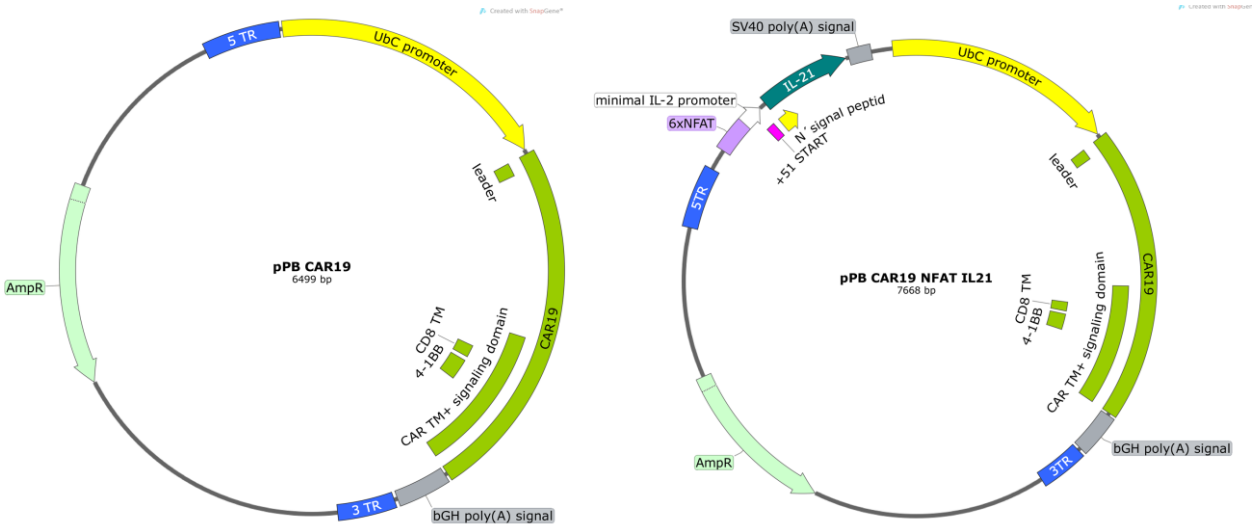

C

The amino acid sequence of PSMA CAR:
MALPVTALLLPLALLLHAARPTREVQLQQSGPELVKPGTSVRISCKTSGYTFTEYTIHWVKQ
SHGKSLEWIGNINPNNGGTTYNQKFEDKATLTVDKSSSTAYMELRSLTSEDSAVYYCAAGW
NFDYWGQGTTVTVSGGGGSGGGGSGGGGSGGGGSDIVMTQSHKFMSTSVGDRVSIICKAS
QDVGTAVDWYQQKPGQSPKLLIYWASTRHTGVPDRFTGSGSGTDFTLTITNVQSEDLADYF
CQQYNSYPLTFGAGTMLEIKREQKLISEEDLNGTTSPTTTPAPRPPTPAPTIASQPLSLRPEAC
RPAAGGAVHTRGLDFACDIYIWAPLAGTCGVLLLSLVITLYCNHRNRRRVKRGRKKLLYIFK
QPFMRPVQTTQEEDGCSCRFPEEEEGGCELRVKFSRSADAPAYQQGQNQLYNELNLGRREE
YDVLDKRRGRDPEMGGKPQRRKNPQEGLYNELQKDKMAEAYSEIGMKGERRRGKGHDG
LYQGLSTATKDTYDALHMQALPPR*

D

The NFAT promoter DNA sequence:

(XhoI)CTCGAGACGCCTTCTGTATGAAACAGTTTTTCCTCCACGCCTTCTGTATGAAACAG

TTTTTCCTCCACGCCTTCTGTATGAAACAGTTTTTCCTCCACGCCTTCTGTATGAAACAGT

TTTTCCTCCACGCCTTCTGTATGAAACAGTTTTTCCTCCACGCCTTCTGTATGAAACAGTT

TTTCCTCCCATTTTGACACCCCCATAATATTTTTCCAGAATTAACAGTATAAATTGCATCTC

TTGTTCAAGAGTTCCCTATCACTCTCTTTAATCACTACTCACAGTAACCTCAACTCCTGCC

CAAGCTTGGCATTCCGGTACTGTTGGTAAAGCCACC(ATG)-->IL21

Fig. S1 The FACS gating strategy and scheme of the CAR vectors.
(A)The dotplots shows the scheme of FACS data analysis. First, cells were gated with a time parameter to remove measurement artifacts, followed with a FSC/SCC gate to remove debris and doublets. Next, live cells CAR+ T cells were identified via Live/Dead Blue dye and with goat anti-mouse Ab. In the case of PSMA CAR T cells we used anti-myc Ab instead of goat anti-mouse Ab. The phenotype was then determined on CD8+ and CD4+ cells by staining for antigens CD62L, CD45RA, CD27, CD28, PD-1. The FMO controls were used to adjust compensations. The image shows a representative sample of CAR19 T cells. (B) The map of CAR19 and CAR19 NFAT IL21 is depicted, the PSMA CAR vectors is identical as CAR19 except for a different scFv. The aminoacid sequence of PSMA CAR is shown in (C) and the DNA sequence of NFAT promoter is shown in (D).

Fig. S2

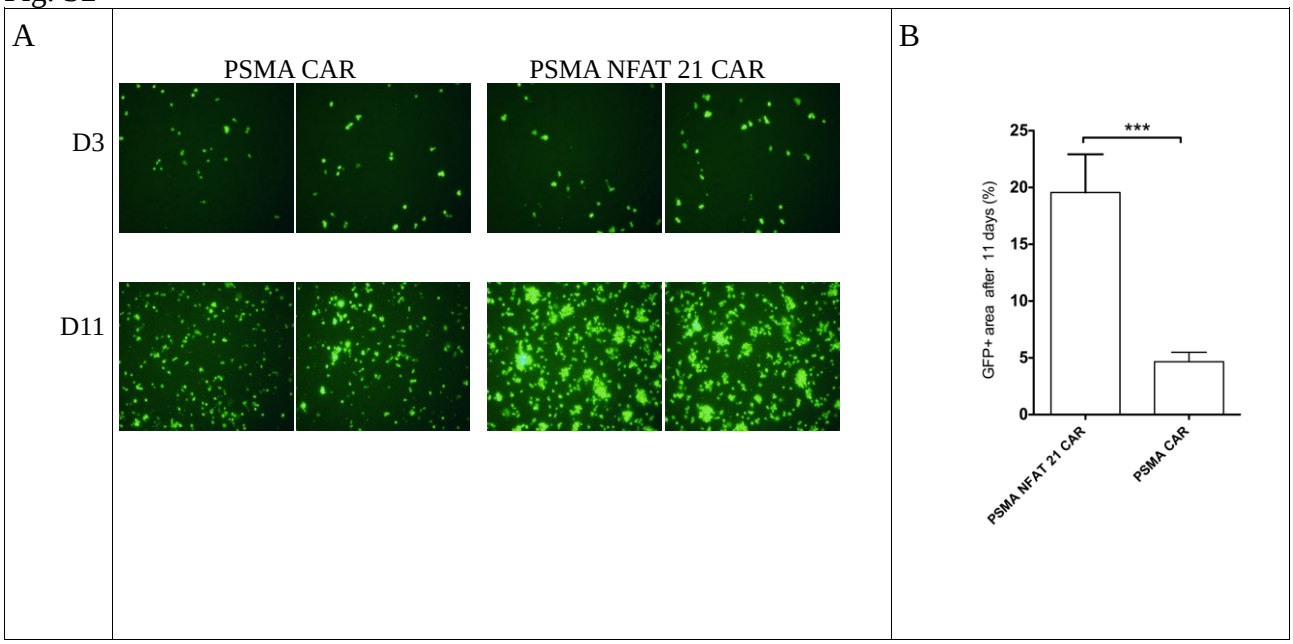

Fig. S2 Inducible secretion of IL-21 increases expansion of PSMA CAR T cells in vitro. (A) PSMA CAR GFP+ T cells, or PSMA NFAT IL-21 GFP+ CAR T were activated with anti-myc Ab and then were expanded in the presence of IL-4, IL-7, IL-21. Manufactured PSMA CAR T cells were then co-cultivated with LNCap cell line under soft agarose. The images show representative two fields of view after 4 days, or 11 days of culture. (B) To quantify the expansion of GFP+ CAR T cells, we used ImageJ software (https://fiji.sc/). First, the image files were converted to 8-bit grayscale. Next a threshold was set as an area outside the cells and all pixels with intensities higher than threshold value were converted to black. The plugin "Analyze Particles" was used to quantify the area containing GFP+ cells. Minimally, four images of randomly chosen fields of view were analyzed. ±SEM, significance was determined with unpaired t test, magnification is 20x. *** $p<0.001$

Fig. S3

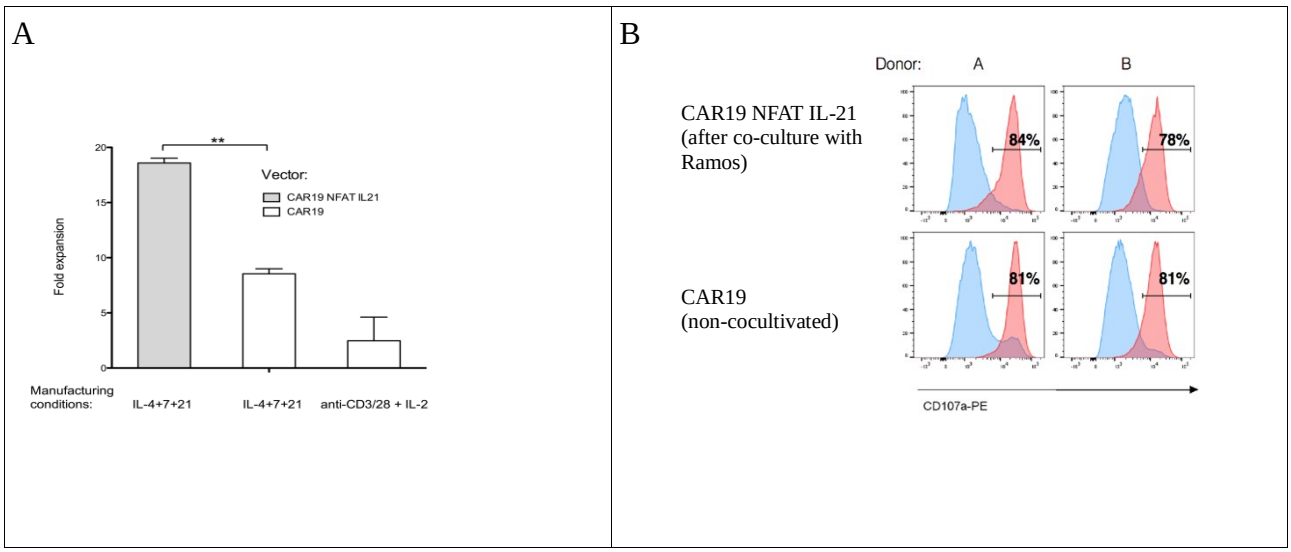

Fig. S3 Inducible secretion of IL-21 increases expansion of functional CAR 19 T cell. (A) CAR19 T cells were manufactured in the presence of IL-4, IL-7, IL-21, or activated by anti-CD3/CD28 Ab's and cultured in the presence of IL-2 , or CAR19 NFAT IL-21 T cells manufactured in the presence of IL-4, IL-7, IL-21 were twice restimulated with Ramos B cells at days 0 and 4. At day 7, the number of CART19 was calculated and is shown as a fold expansion for each sample, the experiment was repeated with almost the same results, n=2, ±SEM, significance was determined with unpaired *t* test. ** $p<0.01$ (B) The histograms show the results of the degranulation assay at the end of experiments. CAR19 NFAT IL-21 are compared to control non-restimulated CAR T cells cultivated in cytokines. Red histograms show the expression of CD107a protein after 4-hour challenge with Ramos cells, blue histograms show the expression of CD107a by non-challenged CAR-T cells.

Fig. S4

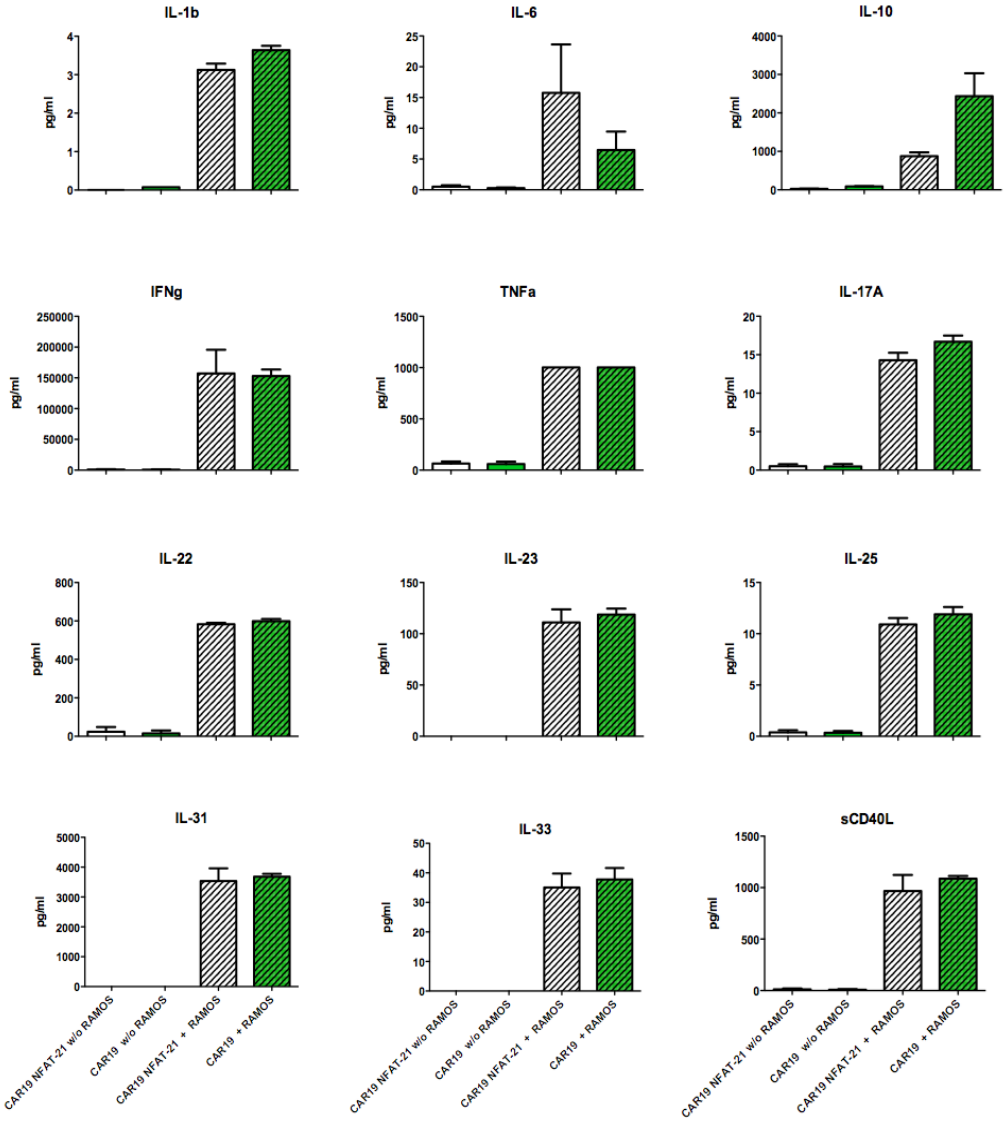

Fig. S4 Production of pro-inflammatory cytokines by CAR19 NFAT-IL21 T cells after antigenic restimulation.
CAR19 NFAT-IL21 or, CAR19 T cells (both were manufactured in IL-4, IL-7, IL-21) were challenged with Ramos B cells (1x10e6 CAR-T + 1x10e6 Ramos in 1 ml media). The amounts of cytokines was then measured in the supernatant after 24 hours via Bio-Plex Human Th17 assay.

Control CAR T cells (designated w/o Ramos) were not challenged with Ramos B cells. The graphs show data from two donors +/- SEM, no significant differences were found between CAR19 NFAT IL-21 and CAR19 T cells.

Fig. S5

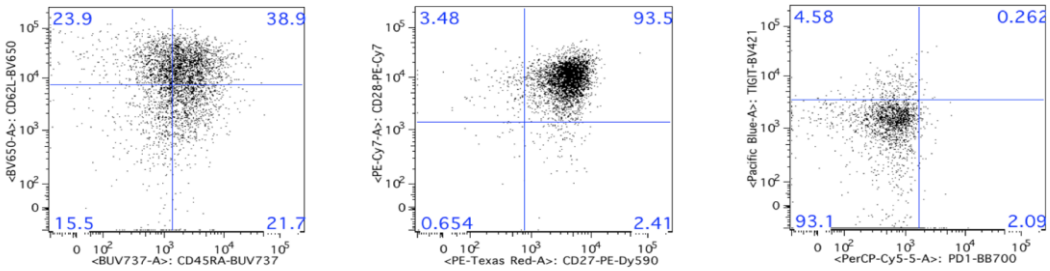

Fig. S5 The immunophenotype of tumor-infiltrating CD19 NFAT IL-21 CAR T cells. NSG mice were transplanted with 5 million of Ramos cells s.c.. After 12 days, when after macroscopic tumors grew out, mice received intravenously 5 million of CAR T cells. 18 days later, mice were sacrificed and the immunophenotype of CD8+ CAR T cells recovered form tumors was determined by FACS by staining for antigens CD8, CD62L, CD45RA, CD28, CD27, PD-1, TIGIT. One representative sample out of six animals is shown. Infiltration of tumors by CAR 19 T cells (non-armed with IL-21) was below the limit of detection and therefore is not shown.

SUPPLEMENTARY MATERIALS FOR PUBLICATION 4

Štach M, Pytlík R, Šmilauerová K, Rychlá J, Mucha M, Musil J, Koladiya A, Nemec M, Petráčková M, Kaštánková I, Pecherková P, Šrámková L, Polgárová K, Trněný M, Lesný P, Vydra J, Otáhal P.

Characterization of the input material quality for the production of tisagenlecleucel by multiparameter flow cytometry and its relation to the clinical outcome.

Pathol Oncol Res. 2023 Apr 20;29:1610914. doi: 10.3389/pore.2023.1610914. PMID: 37151356; PMCID: PMC10156917.

Supplementary table 1

Antibody panel 1

Vendor	Cat#	Antigen	Flurochrome	Clone	Dilution
BD	566460	PD1	BB700	EH12.1	50
Acro Biosystems	FM3-FY45	CAR	FITC	Y45	50
BD	565491	CD3	BV786	UCHT1	50
BD	563808	CD62L	BV650	DREG-56	50
BD	746771	Tim3	BV480	7D3	50
BD	747844	TIGIT	BV421	741182	50
BD	612846	CD45RA	BUV737	HI100	50
BioLegend	302926	CD28	PE-Cy7	CD28.2	50
eBiosciences	61-2239-42	LAG3	PE-eFluor610	3DS223H	40
Exbio	1P-158-T100	CD57	PE	TB01	160
Exbio	T4-308-T100	CD27	APC-Cy7	LT27	25
Exbio	A7-207-T100	CD8	AF700	MEM-31	50
BioLegend	300514	CD4	APC	RPA-T4	50
Invitrogen	L34962	LIVE/DEAD Fixable Blue Dead Cell Stain			

Supplementary table 2

Antibody panel 2

Vendor	Cat#	Antigen	Flurochrome
Exbio custom-made dry reagent	ED7284-1	CD16	FITC
	ED7257-1	CD56	FITC
	ED7507-1	CD14	PerCP-Cy™5.5
	ED7625-1	TCRgd	PE-Cy™7
	ED7133-1	CD19	PE-Cy™7
	ED7162-1	CD3	APC
	ED7140-1	CD4	Pacific Blue
	ED7094-1	CD45	Pacific Orange™
	ED7109-1	CD8	APC-Cy™7
Invitrogen	L34962	LIVE/DEAD Fixable Blue Dead Cell Stain	

Fig. 1S

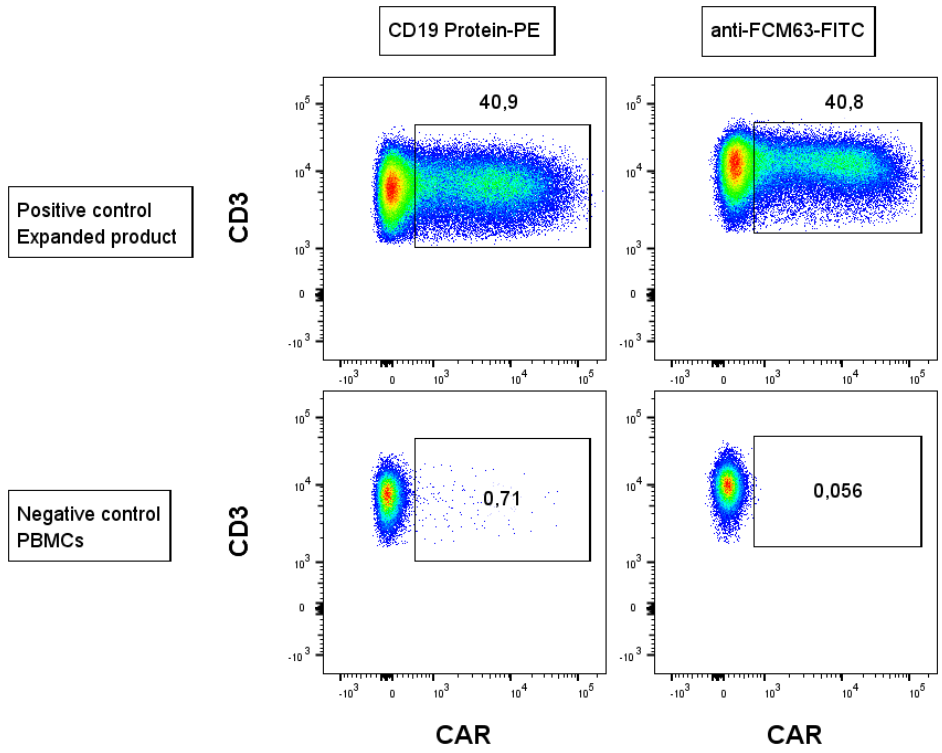

Fig. 1S Comparison between staining with PE-labeled recombinant CD19 protein and FITC-labeled anti-FMC63 antibody, both manufactured by Acro biosystems (catalog numbers CD9-HP254 and FM3-FY45 respectively). As a CAR+ sample, cells from CAR-T product expanded in a cell culture media were used.

Fig 2S

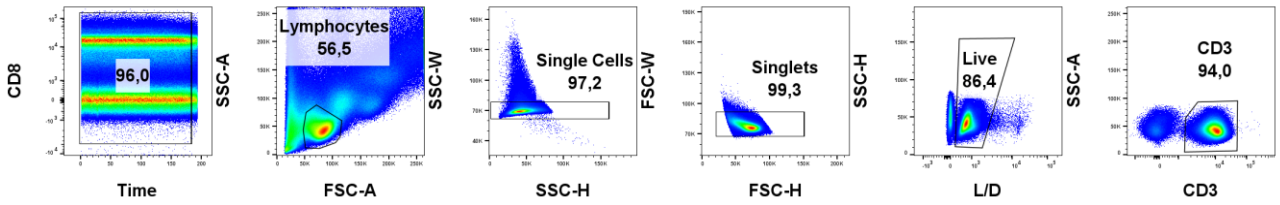

Fig. 2S Pre-gating on CD3+ cells for the phenotype analysis. First, sample integrity was checked on time scale, then lymphocytes were selected, following with single cell gates, live gate and CD3 gate.

Fig. 3S

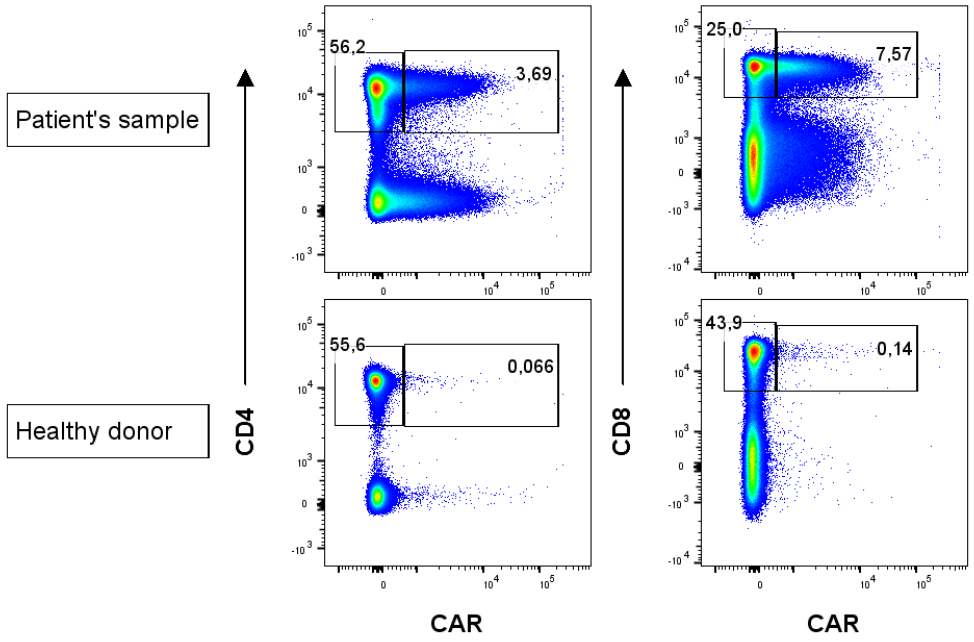

Fig. 3S Gating for CAR-T cells out of CD3+ cells. CAR+ population was determined by using a negative control – healthy donor's sample. Percentages in gates correspond to CAR+ and CAR− populations.

Fig. 4S

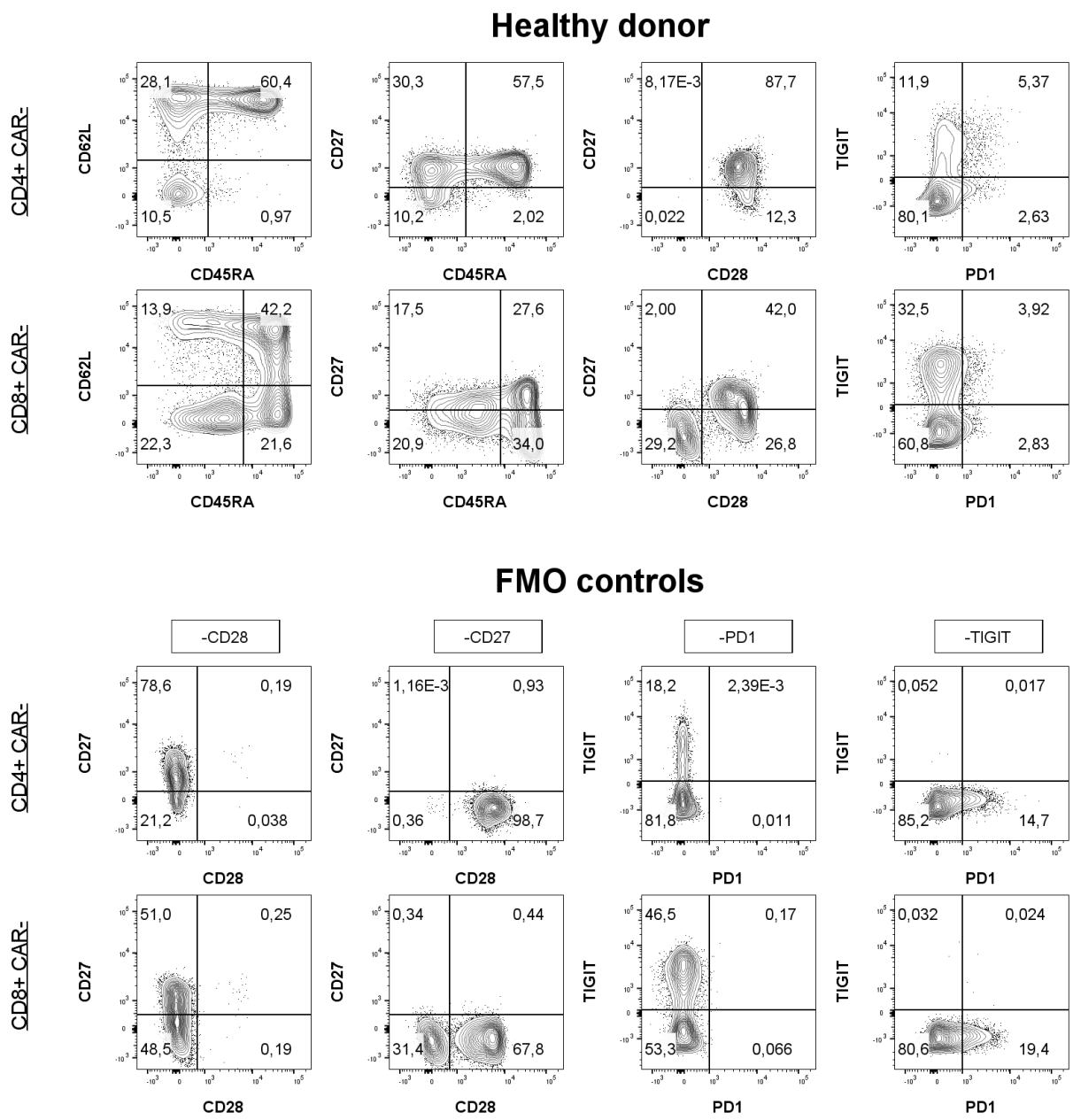

Fig. 4S Gating of T-cell phenotype. CD45RA and CD62L were gated according to healthy donor samples, FMO controls were not reliable for CD8+ cells due to their heterogenic population distribution. CD27, CD28, PD1, and TIGIT were gated according to FMO controls. Percentages are of CD4+ or CD8+ CAR− cells.

Fig. 5S

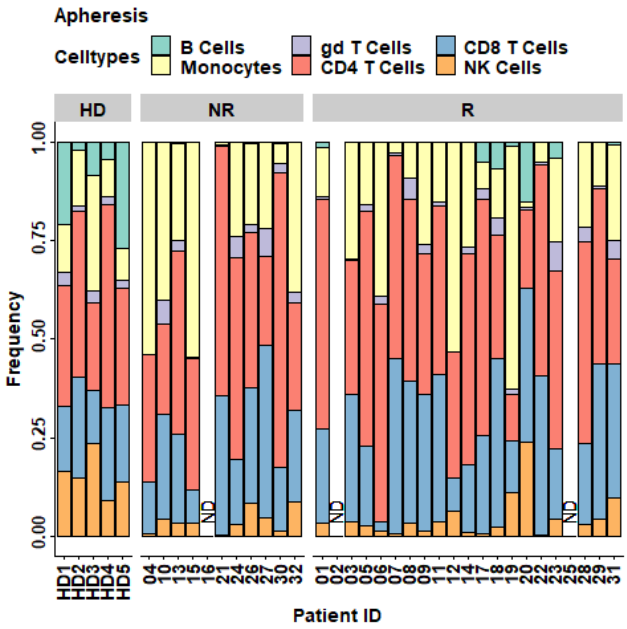

Fig. 5S Composition of leukocyte subsets in apheretic material in individual patients. HD – healthy donors, NR – non-responders, R – responders, ND – not done.

Fig. 6S

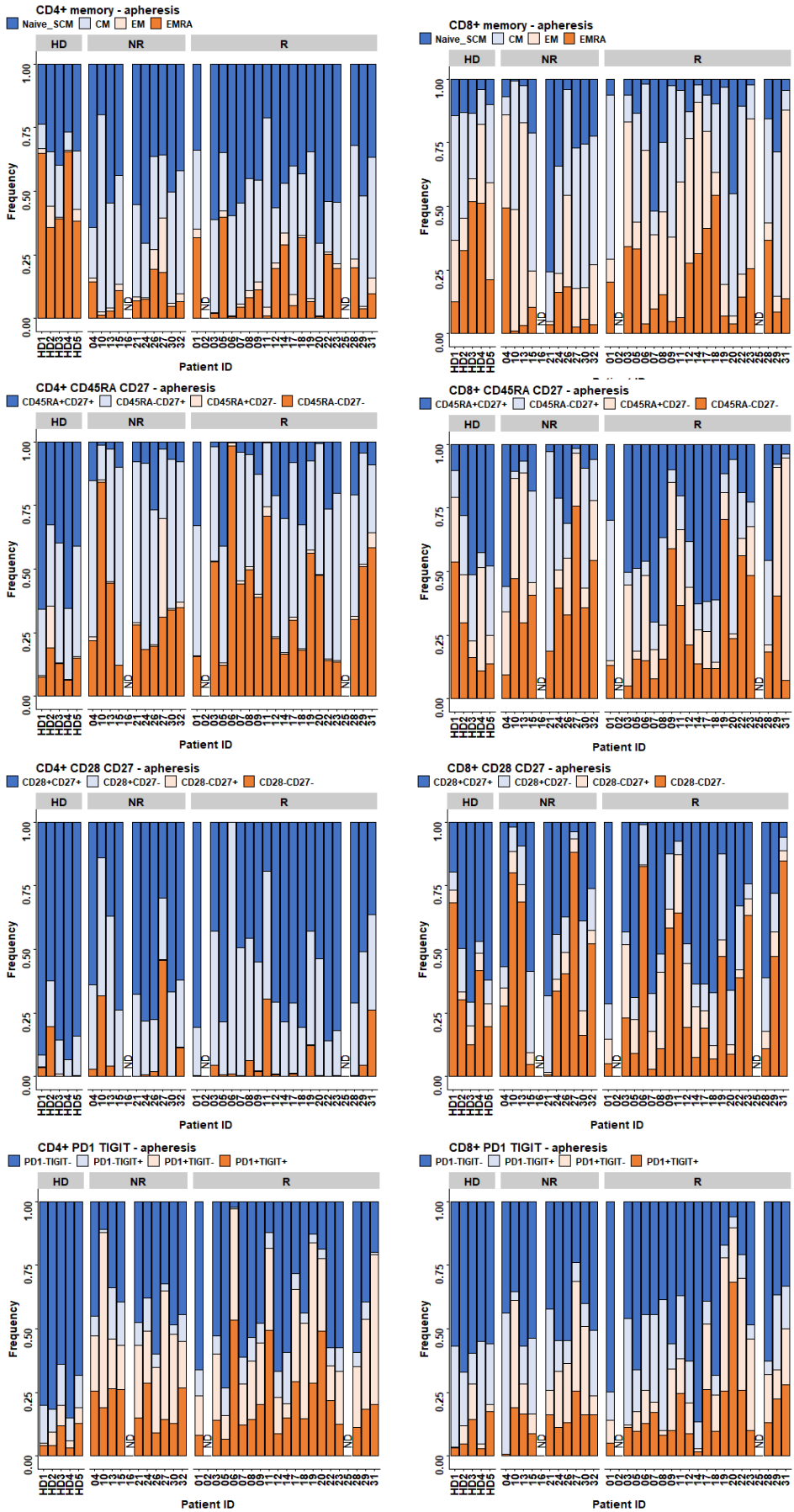

Fig. 6S Immunophenotypes of CD4+ and CD8+ T cells in apheresis of individual patients. HD – healthy donors, NR – non-responders, R – responders, ND – not done.

Fig. 7S

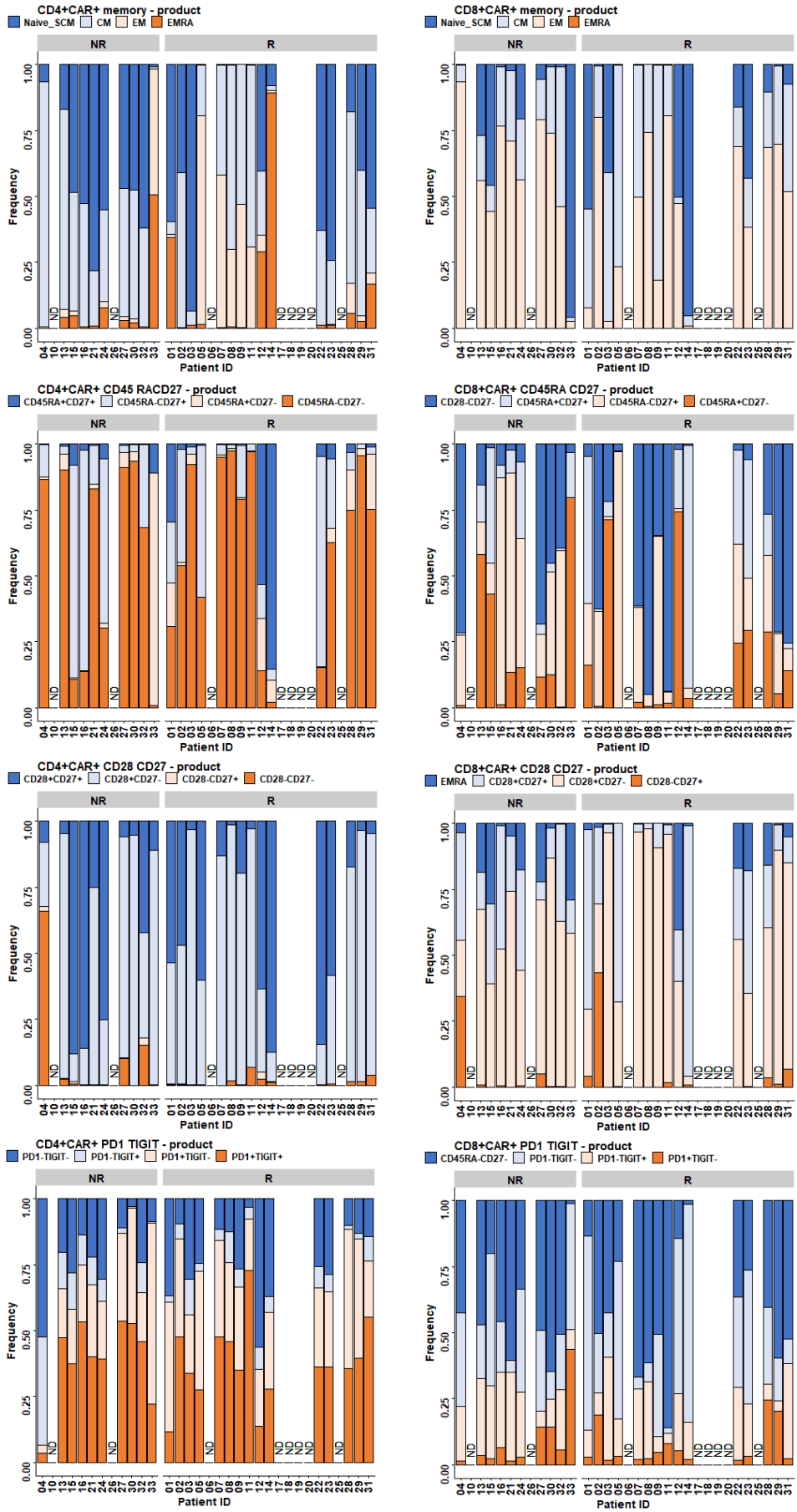

Fig. 7S Immunophenotypes of CD4+CAR+ and CD8+CAR+ T cells in the product for individual patients. NR – non-responders, R – responders, ND – not done.

Fig 8S

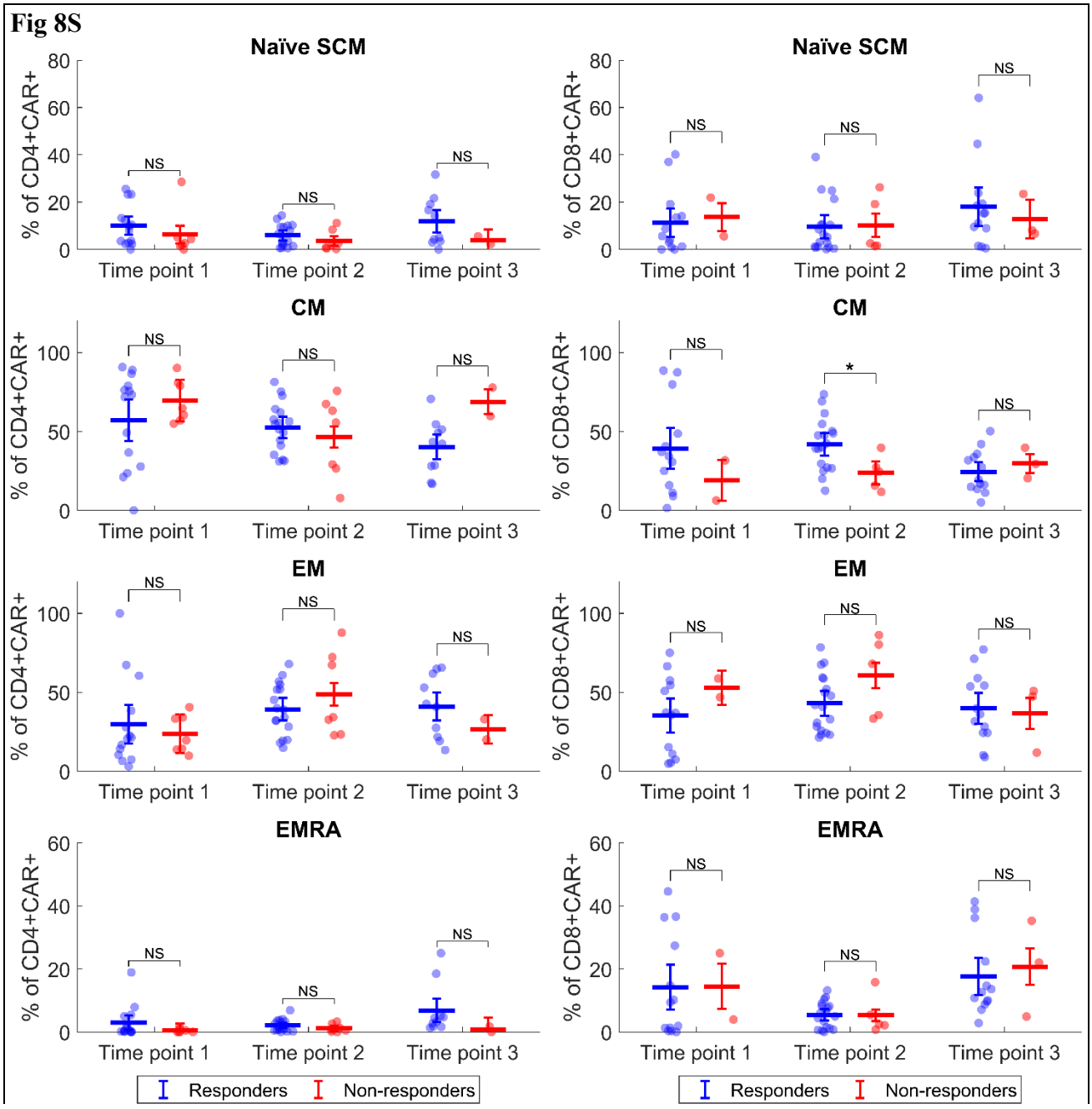
Naïve SCM
% of CD4+CAR+
% of CD8+CAR+
CM
EM
EMRA
NS
*
Time point 1
Time point 2
Time point 3
Responders
Non-responders

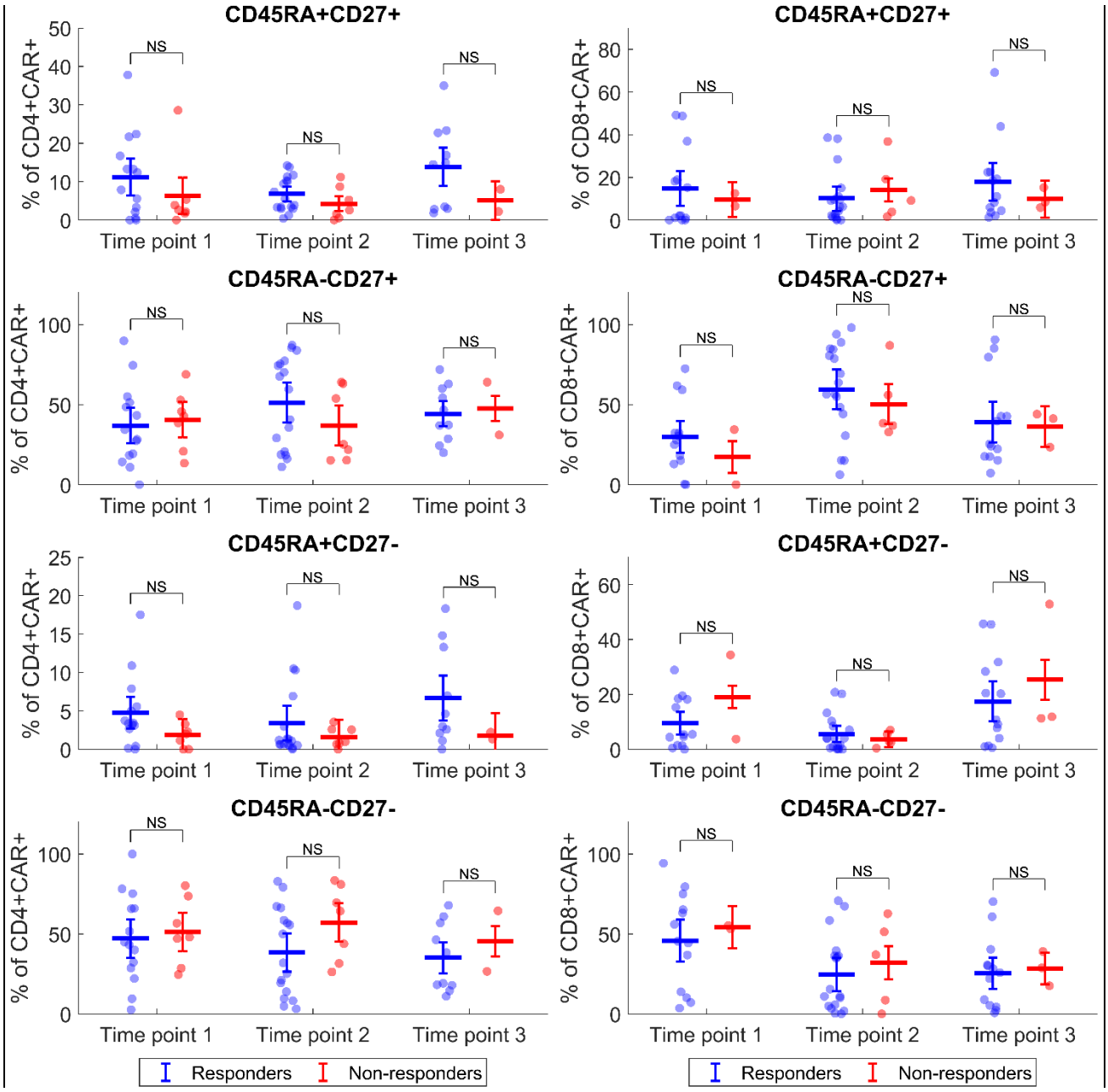
CD45RA+CD27+
% of CD4+CAR+
CD45RA+CD27+
% of CD8+CAR+
CD45RA-CD27+
% of CD4+CAR+
CD45RA-CD27+
% of CD8+CAR+
CD45RA+CD27-
% of CD4+CAR+
CD45RA+CD27-
% of CD8+CAR+
CD45RA-CD27-
% of CD4+CAR+
CD45RA-CD27-
% of CD8+CAR+
NS
Time point 1
Time point 2
Time point 3
Responders
Non-responders

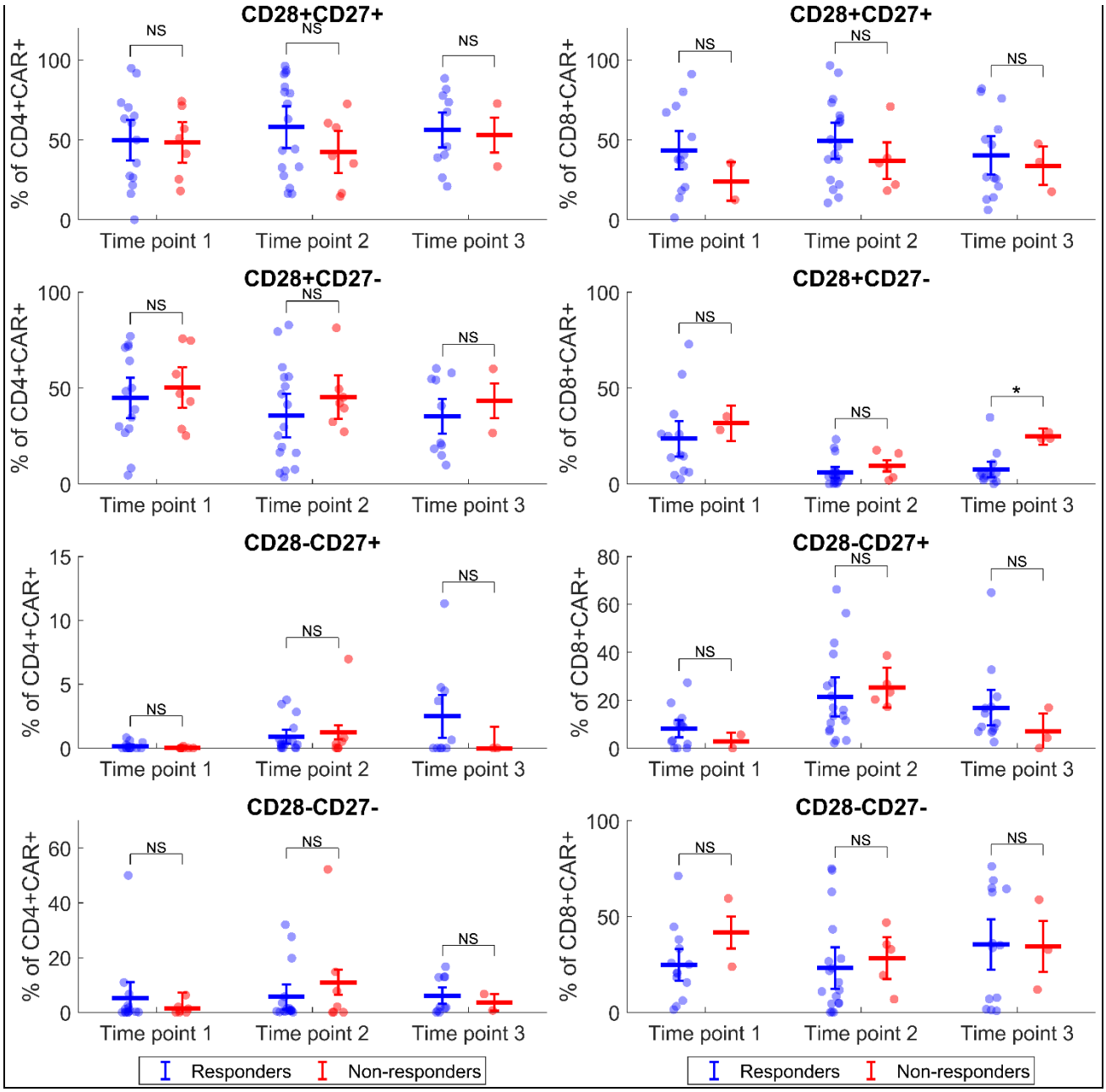
CD28+CD27+
% of CD4+CAR+
% of CD8+CAR+
CD28+CD27-
CD28-CD27+
CD28-CD27-
NS
*
Time point 1
Time point 2
Time point 3
Responders
Non-responders

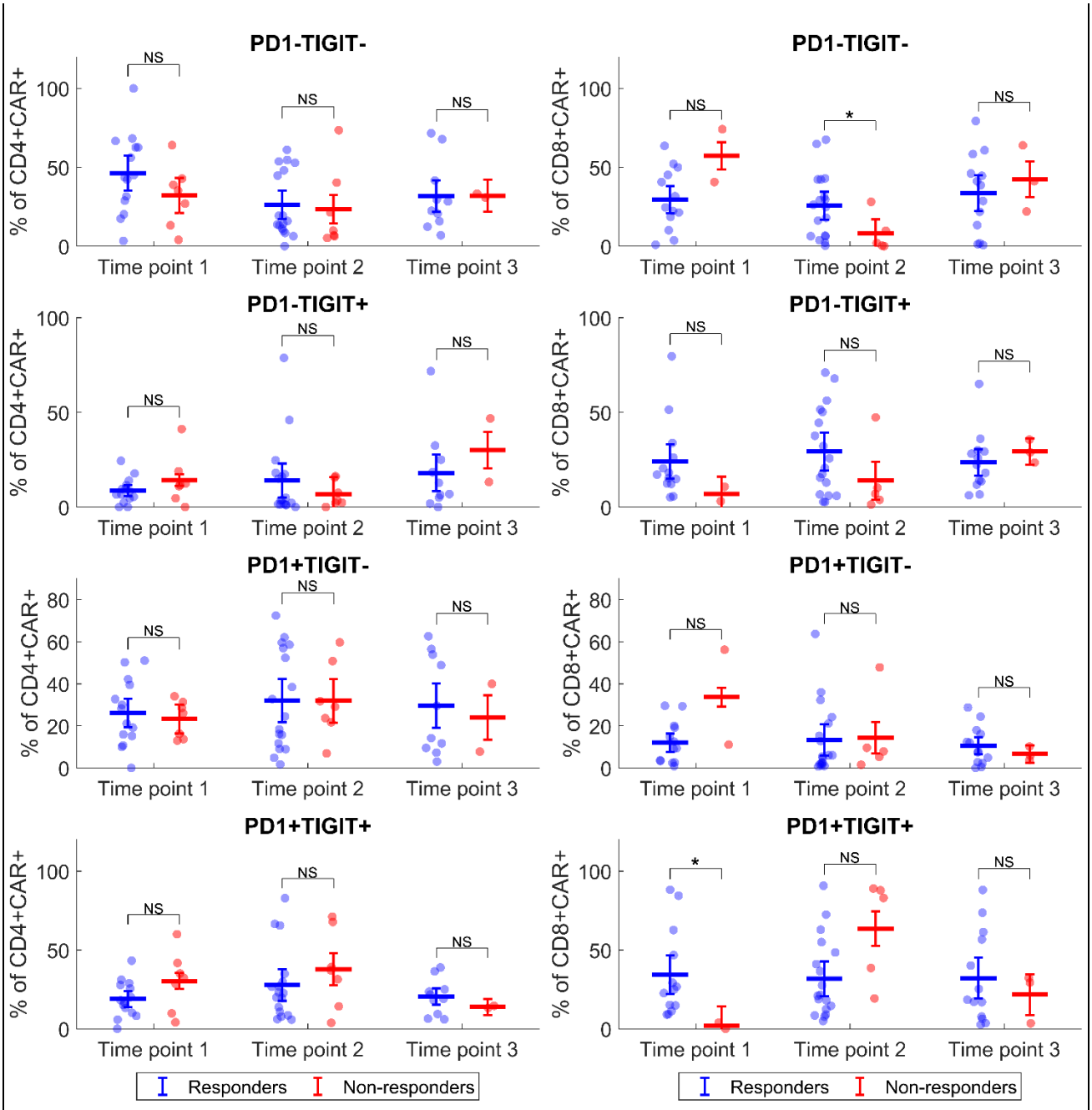

Fig. 8S Immunophenotype of CAR-T cells detected in blood at three time points in responders and non-responders. PD1+TIGIT+ percentage of CD8+CAR+ at time point 1 was higher in responders ($p = 0.048$), however, there were only two samples with detectable CAR-T cells in the non-responders group. Mann-Whitney test, ns - not significant, * $p<0.05$.

Fig. 9S

Bone marrow

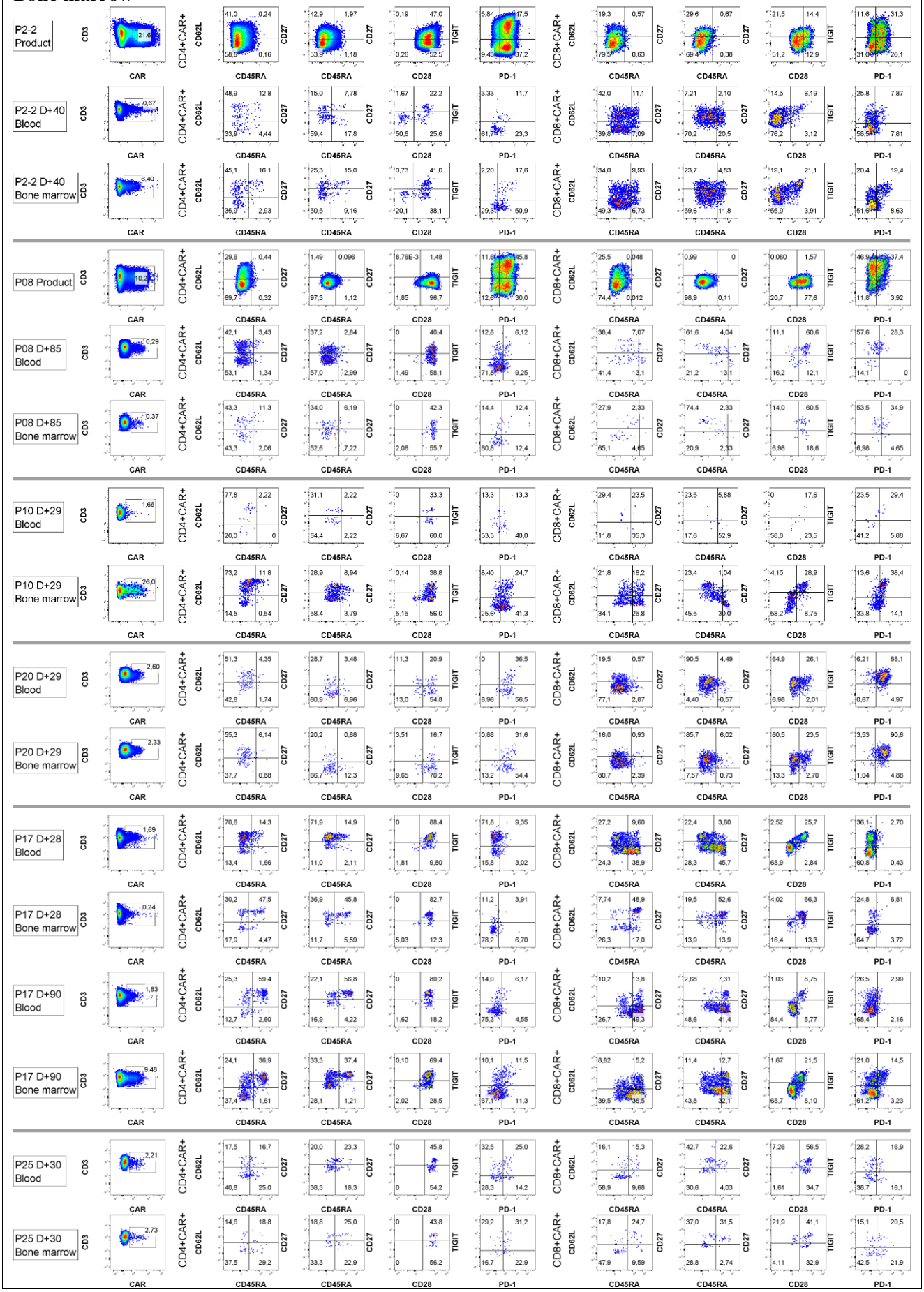

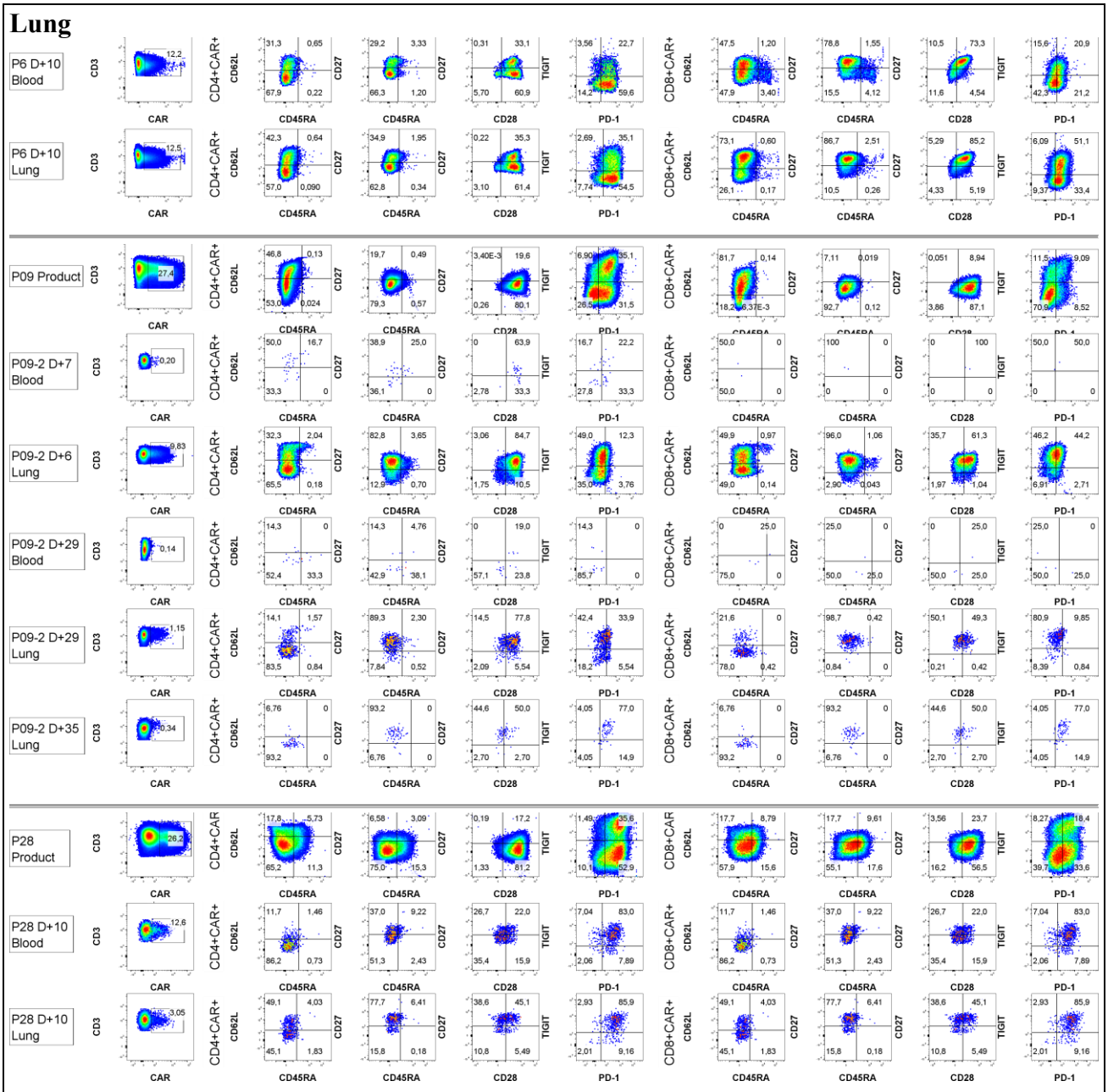

Fig 9S Phenotypes of all bone marrow and lung samples. Only samples with more than 0.1% of CD4+CAR+ or CD8+CAR+ cells are shown. Data for available products are presented for comparison.